# A Near-Infrared Neutral pH Fluorescent Probe for Monitoring Minor pH Changes: Imaging in Living HepG2 and HL-7702 Cells

**ARTICLE** *in* JOURNAL OF THE AMERICAN CHEMICAL SOCIETY · MARCH 2009

Impact Factor: 12.11 · DOI: 10.1021/ja809149g · Source: PubMed

J|A|C|S
ARTICLES

Published on Web 02/06/2009

# A Near-Infrared Neutral pH Fluorescent Probe for Monitoring Minor pH Changes: Imaging in Living HepG2 and HL-7702 Cells

Bo Tang,* Fabiao Yu, Ping Li, Lili Tong, Xia Duan, Ting Xie, and Xu Wang

*College of Chemistry, Chemical Engineering and Materials Science, Engineering Research Center of Pesticide and Medicine Intermediate Clean Production, Ministry of Education, Key Laboratory of Molecular and Nano Probes, Ministry of Education, Shandong Normal University, Jinan 250014, People's Republic of China*

Received November 23, 2008; E-mail: tangb@sdnu.edu.cn

***Abstract:*** A near-neutral pH near-infrared (NIR) fluorescent probe utilizing a fluorophore-spacer- receptor molecular framework that can modulate the fluorescence emission intensity through a fast photoinduced electron-transfer process was developed. Our strategy was to choose tricarbocyanine (Cy), a NIR fluorescent dye with high extinction coefficients, as a fluorophore, and 4′-(aminomethylphenyl)-2,2′:6′,2″-terpyridine (Tpy) as a receptor. The pH titration indicated that Tpy-Cy can monitor the minor physiological pH fluctuations with a p$K_a$ of ∼7.10 near physiological pH, which is valuable for intracellular pH researches. The probe responds linearly and rapidly to minor pH fluctuations within the range of 6.70−7.90 and exhibits strong dependence on pH changes. As expected, the real-time imaging of cellular pH and the detection of pH in situ was achieved successfully in living HepG2 and HL-7702 cells by this probe. It is shown that the probe effectively avoids the influence of autofluorescence and native cellular species in biological systems and meanwhile exhibits high sensitivity, good photostability, and excellent cell membrane permeability.

## Introduction

Intracellular pH plays a pivotal role in many cellular events, including receptor-mediated signal transduction, enzymatic activity,[1] cell growth and apoptosis,[2] ion transport and homeostasis,[3] calcium regulation, endocytosis, chemotaxis, and cell adhesion.[4] Under normal physiological conditions extracellular hydrogen ion concentration is maintained within very narrow limits. The normal value is about 40 nmol/L (pH 7.40) and varies by about 5 nmol/L (pH 7.35−7.45). Deviation by 0.10−0.20 pH units in either direction can cause cardiopulmonary and neurologic problems (e.g., Alzheimer's disease),[5,6] and more extreme variations can be fatal.[6] Hence, $H^+$ is one of the most important targets among the species of interests in vivo. Despite its significance in many essential cellular processes, in vivo pH gradient has not been studied as much as other ions (e.g., $Zn^{2+}$, $Ca^{2+}$) by optical fluorescence probes.[7] Additionally, since fluorescence emission from an indwelling patch can be detected without direct contact, in situ pH measurements can be made noninvasively.[8] Moreover, the fluorescence microscopy provides greater sensitivity and convenience than other invasive methods. These advantages have made fluorescent intracellular pH probes exceptionally suitable for both confocal laser scanning microscopy and flow cytometry.

The requirements of pH sensing have driven the development of several pH probes in the past, such as 1,4-dihydroxyphthalonitrile (1,4-DHPN), 5-(and 6)-carboxyfluorescein, 5-(and 6)-carboxy-4′,5′-dimethylfluorescein, 2′,7′-bis-(2-carboxyethyl)-5-(and 6)-carboxyfluorescein (BCECF), 2′,7′-bis-(2-carboxypropyl)-5-(and 6)-carboxyfluorescein (BCPCF),[9]HPTS (1-hydroxypyrene-3,6,8-trisulfonate),[10] SNAFL (seminaphthofluoresceins),[11] and SNARF (seminaphthorhodafluors).[12] However, the fluorescent

(1) (a) Golovina, V. A.; Blaustein, M. P. *Science* **1997**, *275*, 1643–1648. (b) Kennedy, R. T.; Huang, L.; Aspenwall, C. A. *J. Am. Chem. Soc.* **1996**, *118*, 1795–1796. (c) Clark, H. A.; Kopelman, R.; Tjalkens, R.; Philbert, M. A. *Anal. Chem.* **1999**, *71*, 4837–4843.

(2) (a) Gottlieb, R. A.; Dosanjh, A. *Proc. Natl. Acad. Sci. U.S.A.* **1996**, *93*, 3587–3591. (b) Martinez-Zaguilln, R.; Gillies, R. J. *Cell Physiol. Biochem.* **1996**, *6*, 169–l84. (c) Gottlieb, R. A.; Nordberg, J.; Skowronski, E.; Babior, B. M. *Proc. Natl. Acad. Sci.* **1996**, *93*, 654–658. (d) Gottlieb, R. A.; Giesing, H. A.; Zhu, J. Y.; Engler, R. L.; Babior, B. M. *Proc. Natl. Acad. Sci.* **1995**, *92*, 5965–5968.

(3) (a) Donoso, P.; Beltrán, M.; Hidalgo, C. *Biochemistry* **1996**, *35*, 13419–13425. (b) Hoyt, K. R.; Reynolds, I. J. *J. Neurochem.* **1998**, *7*, 1051–1058. (c) Speake, T.; Elliott, A. C. *J. Physiol.* **1998**, *506*, 415–430. (d) Anderson, R. G. W.; Orci, L. *J. Cell Biol.* **1988**, *106*, 539–543.

(4) (a) Zhao, H.; Xu, X.; Diaz, J.; Muallem, S. *J. Biol. Chem.* **1995**, *270*, 19599–19605. (b) Yuli, I.; Oplatka, A. *Science* **1987**, *235*, 340–342. (c) Levine, S. A.; Nath, S. K.; Chris Yun, H. C.; Yip, J. W.; Montrose, M.; Donowitz, M.; Tse, C. M. *J. Biol. Chem.* **1995**, *270*, 13716–13725. (d) Janecki, A. J.; Montrose, M. H.; Zimniak, P.; Zweibaum, A.; Tse, C. M.; Khurana, S.; Donowitz, M. *J. Biol. Chem.* **1998**, *273*, 8790–8798.

(5) (a) Russell, D. A.; Pottier, R. H.; Valenzeno, D. P. *Photochem. Photobiol.* **1994**, *59*, 309–313. (b) Davies, T. A.; Fine, R. E.; Johnson, R. J.; Levesque, C. A.; Rathbun, W. H.; Seetoo, K. F.; Smith, S. J.; Strohmeier, G.; Volicer, L.; Delva, L. *Biochem. Biophys. Res. Commun.* **1993**, *194*, 537–543. (c) Mogensen, H. S.; Beatty, D. M.; Morris, S. J.; Jorgensen, O. S. *Neuroreport* **1998**, *9*, 1553–1558. (d) Lagadic-Gossmann, D.; Rissel, M.; Galisteo, M.; Guillouzo, A. *Br. J. Pharmacol.* **1999**, *128*, 1673–1682.

(6) Cogan, M. G. *Fluid and Electrolytes*; Appleton and Lange-Prentice Hall Publishers: Norwalk, CT, 1991.

(7) (a) Charier, S.; Ruel, O.; Baudin, J.-B.; Alcor, D.; Allemand, J.-F.; Meglio, A.; Jullien, L. *Angew. Chem., Int. Ed.* **2004**, *43*, 4785–4788. (b) Charier, S.; Ruel, O.; Baudin, J.-B.; Alcor, D.; Allemand, J.-F.; Meglio, A.; Jullien, L. *Chem.−Eur. J.* **2006**, *12*, 1097–1113.

(8) Kermis, H. R.; Kostov, Y.; Harms, P.; Rao, G. *Biotechnol. Prog.* **2002**, *18*, 1047–1053.


10.1021/ja809149g CCC: $40.75 

***Scheme 1***

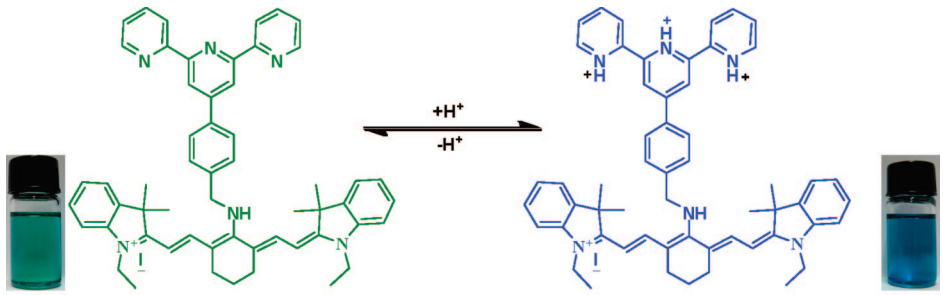


**Tpy-Cy**

pH probes usually suffer from unobvious optical changes in terms of emission spectra variation and fluorescence intensity. The pH probes, reported recently, do not significantly alter the emission spectra too, and the change of fluorescence intensity based on the various pH is no more than 7-fold mostly.[7,13−15] These biological pH probes can be divided into two types: one type is for cytosol which works at a pH of about 6.80−7.40; the other type is for the acidic organelles such as lysosomes and endosomes which functions over the pH range of about 4.50−6.00. Whether the near-neutral ones or the acidic ones, the desirable probes should respond remarkably to a minor pH change, give dependable results, and meanwhile avoid interference from native cellular species particularly. All these will require the fluorescent probe to show good selectivity, high sensitivity, good photostability, and the ability to work within the appropriate pH range. Thus, the focus on this study is to design a near-infrared (NIR, around 650−900 nm) fluorescent pH probe, which can lead to minimum photo damage and can avoid the influence of cell autofluorescence. As far as we know, there is few report on NIR pH fluorescent probes.[16] An acidic NIR pH fluorescent probe had been reported by our group,[17] but no NIR fluorescent probes whose p$K_a$ near neutrality have been found for monitoring pH changes in vivo. Therefore, it is urgent to develop a near-neutral pH NIR fluorescent probe for intracellular pH researches, which is really a bottleneck in cell biological or medical studies. These above reasons have motivated us to develop a new NIR fluorescent intracellular pH probe for sensitively monitoring the near-neutral physiological pH fluctuations to investigate the cellular functions of the compartments.

For solving the problem, our overall strategy is that to choose tricarbocyanine (Cy), a NIR fluorescent dye with high extinction coefficients,[17] as a fluorophore, and 4′-(aminomethylphenyl)-2,2′:6′,2″-terpyridine (Tpy) as a receptor that responds sensitively to $H^+$ near neutrality.[18] We designed and synthesized a new NIR fluorescent probe (Scheme 1) to detect pH in biological systems through a fast photoinduced electron-transfer process (PET). The fluorescence of Tpy-Cy is quenched due to PET between the receptor and the fluorophore, whereas upon N atoms protonation the quenching process is rendered and the fluorescence emission is "switched on".

The pH titration indicates that Tpy-Cy can monitor the minor pH fluctuations with a p$K_a$ of ∼7.10 near physiological pH. The probe responds linearly and rapidly to minor pH fluctuations within the range of 6.70−7.90 and exhibits strong dependence on pH changes. As expected, the real-time imaging of cellular pH and the detection of pH in situ was achieved successfully in living HepG2 and HL-7702 cells by this probe. In addition, the probe effectively avoids the influence of autofluorescence and native cellular species in biological systems and meanwhile, exhibits high sensitivity, good photostability, and excellent cell membrane permeability.

## Experimental Section

**Apparatus.** Fluorescence spectra were obtained with FLS-920 Edinburgh Fluorescence Spectrometer with a Xenon lamp and 1.0-cm quartz cells at the slits of 2.0 /2.0 nm. Absorption spectra were measured on a pharmaspect UV-1700 UV−visible spectrophotometer (SHIMADZU). All pH measurements were performed with a pH-3c digital pH-meter (Shanghai Lei Ci Device Works, Shanghai, China) with a combined glass-calomel electrode. $^1$H and $^{13}$C NMR spectra were taken on a Bruker 300-MHz spectrometer. Determination of organic elements was obtained with Model PE-2400(II) element analyzer. Infrared spectrum was measured with Bruker infrared spectrometer.

**Materials.** 2-[4-Chloro-7-(1-ethyl-3,3-dimethyl(indolin-2-ylidene)]-3,5-(propane-1,3-diyl)-1,3,5-heptatrien-1-yl)-1-ethyl-3,3-dimethyl-3H-indolium (Cy.7.Cl) was synthesized in our laboratory. 4-Me-

(9) (a) Ohkuma, S.; Poole, B. *Proc. Nat Acad. Sci.* **1978**, *5*, 3327–3331. (b) Thomas, J. A.; Buchsbaum, R. N.; Zimniak, A.; Racker, E. *Biochemistry* **1979**, *18*, 2210–2218. (c) Jones, J. M.; Lorton, S. P.; Bavister, B. D. *Cytometry* **1995**, *19*, 235–242. (d) Graber, M. L.; DiLillo, D. C.; Friedman, B. L.; Pastoriza-Munoz, E. *Anal. Biochem.* **1986**, *156*, 202–212. (e) Rink, T. J.; Tsien, R. Y.; Pozzan, T. *J. Cell Biol.* **1982**, *95*, 189–196. (f) Tsien, R. Y. *Methods Cell Biol.* **1989**, *30*, 127–153. (g) Bright, G. R.; Fisher, G. W.; Rogowska, J.; Taylor, D. L. *Methods Cell Biol.* **1989**, *30*, 157–192. (h) Liu, J.; Diwu, Z.; Klaubert, D. H. *Bioorg. Med. Chem. Lett.* **1997**, *7*, 3069–3072.
(10) (a) Clement, N. R.; Gould, J. M. *Biochemistry* **1981**, *20*, 1534–1538. (b) Wolfbeis, O. S.; Furlinger, E.; Kroneis, H.; Marsoner, M. *Anal. Chem.* **1983**, *314*, 119–124. (c) Schulman, S. G.; Chen, S.; Bai, F.; Leiner, M. J. P.; Weis, L.; Wolfbeis, O. S. *Anal. Chim. Acta* **1995**, *304*, 165–170. (d) Zhujun, H.; Seitz, W. R. *Anal. Chem. Acta.* **1984**, *160*, 47–55.
(11) Whitaker, J. E.; Haugland, R. P.; Prendergast, F. G. *Anal. Biochem.* **1991**, *194*, 330–344.
(12) Liu, J. X.; Diwu, Z.; Leung, W.-Y. *Bioorg. Med. Chem. Lett.* **2001**, *11*, 2903–2905.
(13) Sun, K. M.; McLaughlin, C. K.; Lantero, D. R.; Manderville, R. A. *J. Am. Chem. Soc.* **2007**, *129*, 1894–1895.
(14) Galindo, F.; Burguete, M. I.; Vigara, L.; Luis, S. V.; Kabir, N.; Gavrilovic, J.; Russell, D. A. *Angew. Chem., Int. Ed.* **2005**, *44*, 6504–6508.
(15) (a) Ohkuma, S.; Poole, B. *Proc. Natl. Acad. Scd.* **1978**, *75*, 3327–3331. (b) Cui, D. W.; Qian, X. H.; Liu, F. Y.; Zhang, R. *Org. Lett.* **2004**, *6*, 2757–2760. (c) Pal, R.; Parker, D. *Chem. Commun.* **2007**, *47*, 4–476. (d) Lin, H.-J.; Herman, P.; Kang, J. S.; Lakowicz, J. R. *Anal. Biochem.* **2001**, *294*, 118–125.
(16) (a) Jyh-Myng, Z.; Gabor, P. *Anal. Chem.* **1991**, *63*, 2934–2938. (b) Briggs, M. S.; Burns, D. D.; Cooper, M. E.; Gregory, S. J. *Chem. Commun.* **2000**, 2323–2324.
(17) Tang, B.; Liu, X.; Xu, K. H.; Huang, H.; Yang, G. W.; An, L. G. *Chem. Commun.* **2007**, 3726–3728.
(18) Martin, R. B.; Lissfelt, J. A. *J. Am. Chem. Soc.* **1956**, *78*, 938–940.

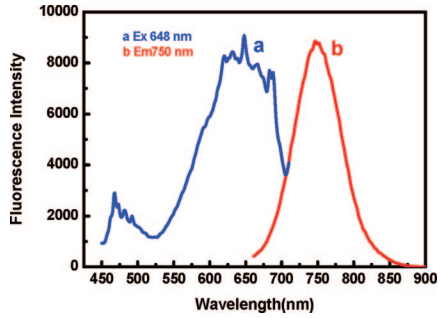


***Figure 1.*** Fluorescence spcetra of Tpy-Cy. The figure shows $\lambda_{max}$ of fluorescence excitation and emission lies in 648 nm (a) and 750 nm (b), respectively.

thylbenzaldehyde, 2-acetylpyridine, and 3-(4,5-dimethylthiazol-2-yl)-2,5-diphenyltetrazolium bromide (MTT) were purchased from Sigma-Aldrich Co. All other chemicals were from commercial sources and of analytical reagent grade, unless indicated otherwise. HepG2 and HL-7702 cells were purchased from the Committee on type Culture Collection of Chinese Academy of Sciences. Ultrapure water was used throughout.

**Absorption Analysis.** Absorption spectra were obtained with 1.0-cm glass cells. The probe Tpy-Cy (0.10 mL, 0.10 mM) was added to a 10.0-mL color comparison tube. After dilution to 1.0 $\mu$M with 40 mM HEPES buffers at various pH values, the mixture was equilibrated for 1 min before measurement. All performancess were carried out in the presence of 0.10 M NaCl to maintain a constant ionic strength.

**Fluorescence Analysis.** Fluorescence emission spectra were obtained with a Xenon lamp and 1.0-cm quartz cells. The probe Tpy-Cy (0.10 mL, 0.10 mM) was added to a 10.0-mL color comparison tube. After dilution to 1.0 $\mu$M with 40 mM HEPES buffers at various pH values, the mixture was equilibrated for 1 min before measurement. The fluorescence intensity was measured simultaneously at $\lambda_{ex/em} = 648/750$ nm. The excitation and emission slits were set to 2.0 and 2.0 nm, respectively. All performs were made in the presence of 0.10 M NaCl to maintain a constant ionic strength.

**In Vivo pH Calibration.** In one set of experiments in $Cl^-$-free solutions, cells were treated with 0.10 mM ouabain for 30 min to increase cellular cytosolic molar sodium ion concentration ($[Na^+]_c$) to high levels. Subsequently these cells in a $Na^+$-free Ringer's solution (to generate $[Na^+]_c > [Na^+]_o$) caused cells to acidify rapidly ($t_{1/2} = 60$ s) from pHc $\approx$ 7.15 to pHc $\approx$ 6.55. Subsequent addition of 100 mM $Na^+$, but not $K^+$, caused cells rapidly to increase pH ($t_{1/2} \approx 10$ s) toward the control value. These changes of pH were blocked when ouabain-treated cells had been pre-equilibrated for 10 min with 1 mM amiloride, and this block was overcome by adding 10 $\mu$M monensin (an ionophore that artificially exchanges $Na^+$ for $H^+$). In another set of experiments in $Cl^-$-containing Ringer's solution, when ammonium chloride ($NH_4Cl$ 20 mM) was used, 20 mM NaCl was removed from the medium in order to avoid any change of osmotic force. $NH_4Cl$ was added to solutions shortly before use. Addition and then (about 4 min) removal of $NH_4Cl$ was used to induce an acid load in order to activate the pH-regulatory mechanisms. Calibration solutions used in this study have been described elsewhere.[66,19]

**MTT Assay.** HL-7702 cells ($10^6$ cell $mL^{-1}$) were dispersed within replicate 96-well microtiter plates to a total volume of 200 $\mu$L $well^{-1}$. Plates were maintained at 37 °C in a 5% $CO_2$/95% air incubator for 4 h. HL-7702 cells were then incubated for 24 h upon different concentrations probe of $10^{-3}$, $10^{-4}$, $10^{-5}$, $10^{-6}$, $10^{-7}$, and $10^{-8}$ M, respectively. MTT (Sigma) solution (5.0 mg $mL^{-1}$, HEPES) was then added to each well. After 4 h, the remaining MTT solution was removed, and 150 $\mu$L of DMSO was added to each well to dissolve the formazan crystals. Absorbance was measured at 490 nm in a TRITURUS microplate reader. Calculation of IC50 values was done according to Huber and Koella.[20]

**Confocal Imaging.** Florescent images were acquired on a LSM510 confocal laser-scanning microscope (Carl Zeiss Co., Ltd.) with an objective lens ( $\times$40). The excitation wavelength was 633

***Scheme 2***

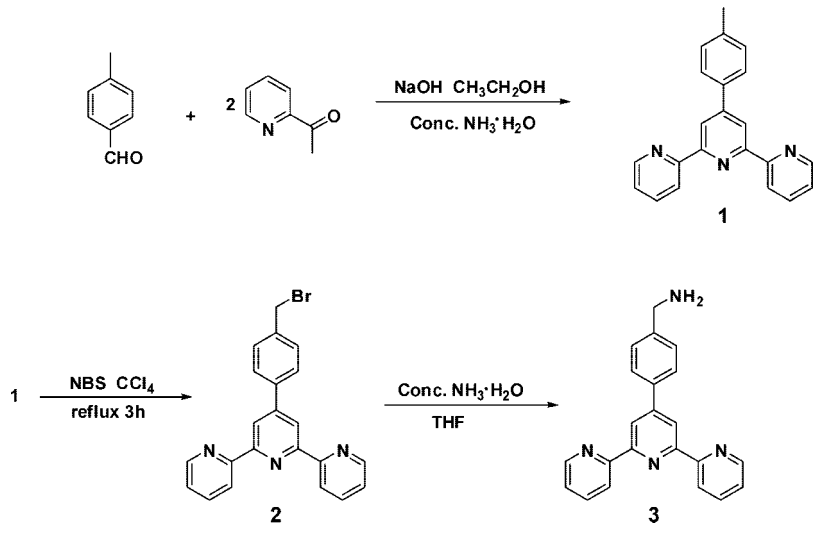


***Scheme 3***

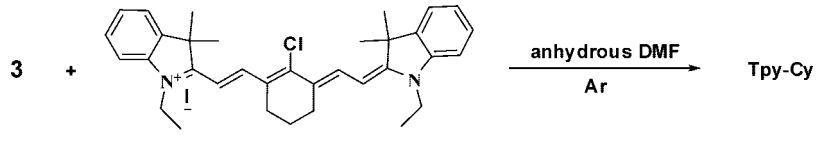


**Cy.7.Cl**

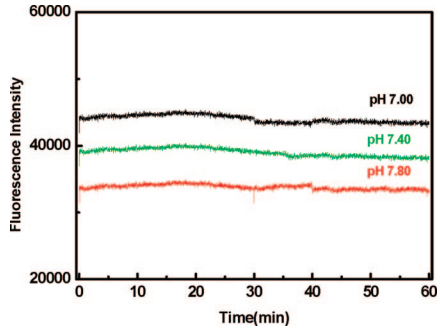


***Figure 2.*** Time course of the Tpy-Cy were measured by spectrofluorometer ($\lambda_{ex}$ = 648 nm and $\lambda_{em}$ = 750 nm). The concentration of Tpy-Cy was 3.0 $\mu$M in 40 mM HEPES buffer pH 7.00, 7.40, and 7.80, respectively.

nm. Prior to imaging, the medium was removed. Cell imaging was carried out after washing cells with HEPES (0.10 M) for three times.

**Cell Culture.** Human hepatocellular liver carcinoma cell line (HepG2) and human hepatocyte cell line (HL-7702) were maintained following protocols provided by the American type Tissue Culture Collection. Cells were seeded at a density of $1 \times 10^6$ cells $mL^{-1}$ for confocal imaging in RPMI 1640 Medium supplemented with 10% fetal bovine serum (FBS), $NaHCO_3$ (2 g/L), and 1% antibiotics (penicillin /streptomycin, 100 U/ml). Cultures were maintained at 37 °C under a humidified atmosphere containing 5% $CO_2$.

**Synthesis and Characterization of Tpy Cy.** Our optimization of the one-step reaction started from readily available aryl aldehydes and 2-acetylpyridine (Scheme 2). The enolate of 2-acetylpyridine can be generated by NaOH under mild conditions.[21] The following aldol condensation and Michael addition proceeded smoothly at room temperature. The soluble diketone intermediate was then allowed to form the central pyridine ring with an aqueous ammonia nitrogen source. In theory, ammonia can undergo the $S_N2$ reaction with alkyl halides to produce a range of primary, secondary, and tertiary amines. The synthesis of 4′-(aminomethylphenyl)-2,2′:6′,2″-terpyridine (**3**) (Scheme 2) was very straightforward using this mild condition.

**4′-(Aminomethylphenyl)-2,2′:6′,2″-terpyridine (1).** 2-Acetylpyridine (4.84 g, 40 mmol) was added into a solution of 4-methylbenzaldehy (2.40 g, 20 mmol) in EtOH (100 mL). KOH pellets (3.08 g, 85%, 40 mmol) and aq $NH_3$ (60 mL, 29.3%) were then added to the solution. The solution was stirred at 34 °C for 24 h. The mixture was cold to 20 °C, and then the off-white solid was collected by filtration and washed with ice-cold EtOH (10 mL). Recrystallization from EtOH afforded white crystalline solid **1** (4.2 g, 13.0 mmol, 65%). mp 164−165 °C. $^1$H NMR (300 MHz, $CDCl_3$): $\delta$(ppm) = 2.44 (s, 3 H), 7.37 (dd,2 H), 7.54 (d,), 7.90 (mc, 4 H), 8.68 (d), 8.74 (mc, 4 H). $^{13}$C NMR ($CDCl_3$, 75 MHz) $\delta$(ppm): 156.2, 155.6, 150.3, 148.9, 139.1, 137.0, 135.4, 129.6, 127.2, 123.8, 121.5, 118.8, 21.2. Elemental Analysis: Calcd C, 81.7; H, 5.3; N, 13.0. Found C, 81.7; H, 5.3; N, 13.0.

**4′-(4-Bromomethylphenyl)-[2,2′:6′,2″]terpyridine (2).** A mixture of 4′-(methylphenyl)-2,2′:6′,2″-terpyridine (5.0 g, 15.5 mmol), *N*-bromsuccinimide (NBS, 3.3 g, 18.5 mmol), and α,α′-azoisobutyroniltrile (AIBN, 0.2 g, 1.2 mmol) in dry $CCl_4$ (50 mL) was refluxed for 2 h. The warm reaction mixture was filtered to remove the succinimide, and the solvent was evaporated. The crude product was recrystallized from EtOH to give **2** as a pale-yellow solid (yield: 5.59 g, 90%). mp 152−153 °C. $^1$H NMR ($CDCl_3$, 300 MHz) $\delta$(ppm): 4.75 (s, 2 H), 7.37 (dd, 2 H), 7.54 (d,), 7.90 (mc, 4 H), 8.68 (d), 8.74 (mc, 4 H). $^{13}$C NMR($CDCl_3$, 75 MHz) $\delta$(ppm): 155.3, 149.6, 148.9, 148.6, 138.7, 138.4, 138.2, 137.6, 137.3, 129.6, 129.2, 128.1, 127.8, 121.7, 121.5, 119.2, 29.7. Elemental Analysis: Calcd C, 65.7; H, 4.0; Br, 19.9; N, 10.6. Found C, 65.7; H, 4.0; Br, 19.9; N, 10.6.

**4′-(Aminomethylphenyl)-2,2′:6′,2″-terpyridine (3).** THF (40 mL) and $NH_3$ (80 mL, 29.3%) were added in a 250-mL round-bottom flask. Then the mixture was stirred at 25 °C. **2** (1 g, 2.5 mmol) was dissolved in 80 mL of THF and was added in the flask drop by drop within 4 h by constant pressure funnel; the reaction was continued for another 4 h. The organic phase was dried over $MgSO_4$. The solvent was evaporated, and the product **3** (yield: 0.79 g, 93%) was given as a light yellow solid, and the crude product need not further purification. mp 99−100 °C. $^1$H NMR ($CDCl_3$, 300 MHz) $\delta$(ppm): 4.36(s,2H), 7.37 (dd,2 H), 7.54 (d,), 7.90 (mc, 4 H), 8.61(s,2H), 8.68 (d), 8.74 (mc, 4 H). $^{13}$C NMR ($CDCl_3$, 75 MHz) $\delta$(ppm): 156.3, 156.1, 155.9, 150.0, 149.5, 149.1, 140.7, 140.2, 138.2, 137.2, 136.8, 129.9, 128.8, 128.6, 128.3, 127.9, 127.8, 127.3, 123.7, 121.3, 118.8, 51.2. GC-MS (API-ES): *m*/*z* Calcd 338.4, found 338.1 $[M]^+$. Elemental Analysis: Calcd C, 78.0; H, 5.4; N, 16.6. Found C, 77.8; H, 5.5; N, 16.5.

**2-{4-[4′-(Aminomethylphenyl)-2,2′:6′,2″-terpyridinyl]-7-(1-ethyl-3,3-dimethyl(indolin-2-ylidene)}-3,5-(propane-1,3-diyl)-1,3,5-heptatrien-1-yl)-1-ethyl-3,3-dimethyl-3H-indolium (Tpy-Cy).** 1.00 g (0.156 mmol) of Cy and 0.5279 g (1.56 mmol) of **3** were dissolved in 20 mL of anhydrous DMF in a 50-mL round-bottom flask (Scheme 3). The mixture was stirred at 90 °C under Ar for 24 h.[17] Then the solvent was evaporated on a rotary evaporator until dry. The solid was purified on silica gel chromatography eluted with ethyl acetate/methanol (1:3 v/v). $^1$H NMR (300 MHz, DMSO-$D_6$) $\delta$(ppm): 1.38−1.54(m, 22H), 1.98(s, 1H), 2.71(s, 2H), 2.87(s, 2H), 3.84(s, 2H), 4.41(d, 2H), 5.17(s, 1H), 5.64(s, 1H), 5.80(m, 1H), 6.23(m, 1H), 7.52−8.18(m, 14H), 8.51−8.76(m, 7H), 10.12(s, 1H). $^{13}$C NMR (DMSO-$D_6$, 75 MHz) $\delta$(ppm): 162.8, 161.7, 156.1, 155.4, 149.7, 141.6, 140.9, 140.3, 137.9, 136.5, 130.8, 130.1, 128.7, 128.2, 127.3, 127.1 125.0, 121.4, 118.6,118.2, 82.4, 60.8, 58.4, 54.3, 49.0, 42.2, 40.7,40.2,40.0, 39.1, 36.2, 32.6, 31.2, 29.1, 28.2, 11.7. GC-MS (API-ES): *m*/*z* Calcd 813.5, found 813.6 $[M]^+$. Elemental Analysis: Calcd C, 71.4; H, 6.1; I, 13.4; N, 8.93. Found C, 71.5; H, 6.1; I, 13.5; N, 8.9.

## Results and Discussion

**Fluorescence Spectra.** Fluorescence spectral property of Tpy-Cy was examined in buffered aqueous solution (40 mM HEPES, Tpy-Cy 3.0 $\mu$M, pH 7.40). The probe showed $\lambda_{max}$ of excitation and emission lies in 648 and 750 nm respectively.

**Kinetic Assays.** The stability of the probe was tested by measuring the fluorescent response during 1 h. Figure 2 shows the time courses of fluorescence intensity of the probe (3.0 $\mu$M) in 40 mM buffer solution with pH 7.00, 7.40, and 7.80 at room temperature. The fluorescence intensity was measured simultaneously at $\lambda_{ex/em}$ = 648/750 nm. The experiment indicates that the probe can instantly respond to the change of $H^+$ concentration, and the probe solution is stable to the medium, light, and air.

**Standard Fluorescence pH Titrations.** Standard fluorescence pH titrations were performed in buffer solution at a probe concentration of 1.0 $\mu$M. It is interesting that Tpy-Cy undergoes distinct color change from blue to green (Scheme 1 and Figure 3c). Parts a and b of Figure 3 show the pH dependence on the emission spectrum of Tpy-Cy that now displays fluorescent pH-sensing activity in the physiological pH range. Furthermore the change of fluorescence intensity based on the pH variation is over 30-fold (Figure 3b). Compared with the reported ones,[7,13−15,22]

(19) (a) Paradiso, A. M.; Tsien, R. Y.; Machen, T. E. *Proc. NatI. Acad. Sci. U.S.A.* **1984**, *81*, 7436–7440. (b) Llopis, J.; Michael Mccaffery, J.; Miyawaki, A.; Farquhar, M. G.; Tsien, R. Y. *Proc. Natl. Acad. Sci.* **1998**, *95*, 6803–6808.
(20) Huber, W.; Koella, J. C. *Acta Trop.* **1993**, *55*, 257–261.
(21) (a) Wang, J. H.; Hanan, G. S. *Synlett.* **2005**, *8*, 1251–1254. (b) Winter, A.; Egbe, D. A. M.; Schubert, U. S. *Org. Lett.* **2007**, *9*, 2345–2348. (c) Cargill Thompson, A. M. W. *Coord. Chem. Rev.* **1997**, *160*, 1–52. (d) Spahi, W.; Calzaferri, G. *Helv. Chem. Acta.* **1984**, *67*, 450–454.

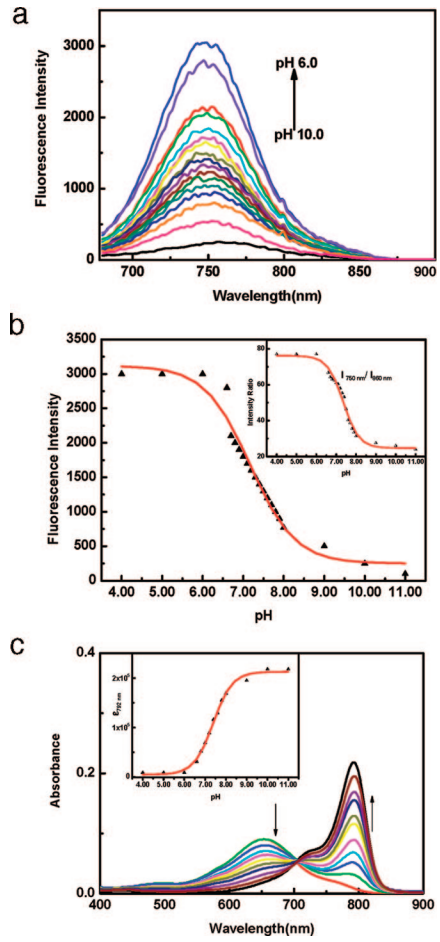


***Figure 3.*** (a) The fluorescence emission changes at 750 nm with the pH titration curve of Tpy-Cy (1.0 $\mu$M), pH 6.00, 6.60, 6.70, 6.80, 6.90, 7.00, 7.10, 7.20, 7.30, 7.40, 7.50, 7.60, 7.70, 7.80, 7.90, 8.00, 9.00, and 10.00 (40 mM buffer solution, 0.10 M NaCl). (b) Fluorescence responses of Tpy-Cy (1.0 $\mu$M) to different pH: 4.00, 5.00, 6.00, 6.60, 6.70, 6.80, 6.90, 7.00, 7.10, 7.20, 7.30, 7.40, 7.50, 7.60, 7.70, 7.80, 7.90, 8.00, 9.00, 10.00, and 11.00. Spectras were obtained with excitation at 648 nm and emission at 750 nm in buffered aqueous solution (40 mM HEPES). Inset: Ratiometric calibration curve of $I_{750\ nm}/I_{860\ nm}$ (intensity at 750 nm vs intensity at 860 nm). (c) Dependence on pH of the absorption in buffered aqueous solution (from acidic to basic conditions: pH 6.00, 6.60, 6.80, 7.00, 7.20, 7.40, 7.60, 7.80, 8.00, 9.00, 10.00). Inset: nonlinear fitting of the pH-dependent extinction coefficient $\epsilon_{792nm}$.

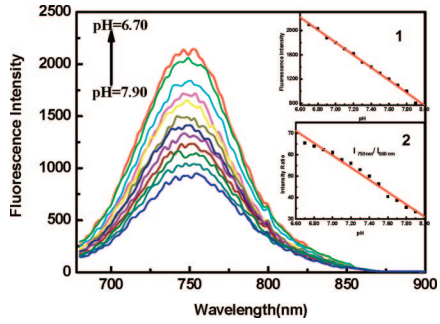


***Figure 4.*** Fluorescence responses of Tpy-Cy (1.0 $\mu$M) to different pH: 6.70, 6.80, 6.90, 7.00, 7.10, 7.20, 7.30, 7.40, 7.50, 7.60, 7.70, 7.80, and 7.90. Spectra were obtained with excitation at 648 nm ranging from 680 to 900 nm in buffered aqueous solution. Inset 1: The relationship between fluorescence intensity and pH. Inset 2: The relationship of fluorescence intensity ratio ($I_{750\ nm}/I_{860\ nm}$) and pH.

our NIR probe wins out in responding highly sensitively to a minor pH change and possessing a near-neutral p$K_a$ of 7.10.

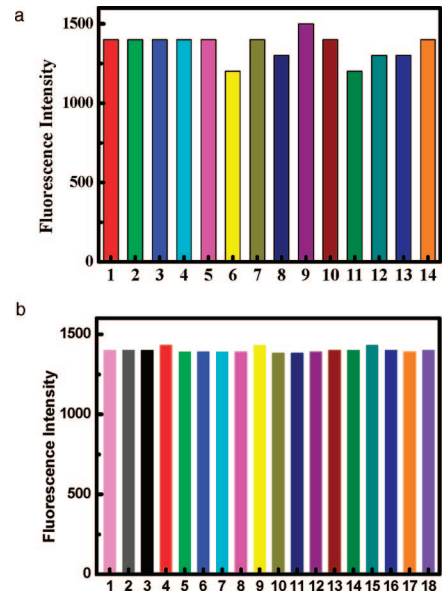


***Figure 5.*** (a) Fluorescence responses of 1.0 $\mu$M Tpy-Cy in HEPES (40 mM pH 7.40) to diverse ions. 1, blank; 2, $K^+$ (120 mM); 3, $Na^+$ (120 mM); 4, $Ca^{2+}$ (0.5 mM); 5, $Mg^{2+}$ (0.5 mM); 6, $Zn^{2+}$ (0.3 mM); 7, $Pb^{2+}$ (0.3 mM); 8, $Cu^{2+}$ (0.3 mM); 9, $Mn^{2+}$ (0.3 mM); 10, $Hg^{2+}$ (0.3 mM); 11, $Ag^+$ (0.3 mM); 12, $Co^{2+}$ (0.3 mM); 13, $Ni^{2+}$ (0.3 mM); 14,$Cd^{2+}$ (0.3 mM). All data were obtained after incubation at room temperature for 20 min. (b) Fluorescence responses of 1.0 $\mu$M Tpy-Cy in HEPES (40 mM pH 7.40) to proteins and bioactive small molecules. 1, blank; 2, glutathione (100 $\mu$M); 3, L-cysteine (100 $\mu$M); 4, vitamin C (100 $\mu$M); 5, glycine (100 $\mu$M); 6,: proline (100 $\mu$M); 7, tyrosine (100 $\mu$M); 8, tryptophan (100 $\mu$M); 9, glutamic acid (100 $\mu$M); 10, histidine (100 $\mu$M); 11, arginine (100 $\mu$M); 12, dopamine (100 $\mu$M); 13, L-adrenaline (100 $\mu$M); 14, HQ (100 $\mu$M); 15, uric acid (100 $\mu$M); 16, thioredoxin (50 $\mu$M); 17, glutathione reductase (50 U/mg protein); 18, metallothionein (100 $\mu$M). All data were obtained after incubation at room temperature for 20 min.

With changing the fluorescence intensity, there is hardly influence on $\lambda = 860$ nm. Therefore, the ratio of the fluorescence intensity at peak wavelength ($\lambda = 750$ nm) vs wavelength $\lambda = 860$ nm is constant regardless of the change of fluorophore concentration by photobleaching or change of the external environment.[23] The ratiometric data in various pH are provided (Figure 3b). According to Figure 3c, the molar extinction coefficient $\epsilon$ can now be obtained by using Lambert−Beer's law. Acid form: $\epsilon_1 = 121000$ L mol $^{-1}$ cm$^{-1}$ ($\lambda_{max} = 650$ nm pH 6.00). Alkaline form: $\epsilon_2 = 218000$ L mol $^{-1}$ cm$^{-1}$ ($\lambda_{max} = 792$ nm pH 10.00). The fluorescence quantum yield of Tpy-Cy was also studied. In pH 10.00 buffer, the fluorescence intensity was very low $\Phi = 0.008$, which was determined in methanol in reference to rhodamine B ($\Phi_f = 0.69$ in methanol).[24] The low quantum yield of Tpy-Cy resulted from PET quenching of the Cy emission by lone pair electrons of Tpy. Whereas upon N atoms protonation the quenching process was rendered, strong fluorescence was obtained immediately. The fluorescence quantum yield increased to 0.13.

**Determination of $K_a$ from Fluorimetric Titration.** In view of the structure of the probe, the molecule contains three basic sites, probably with close protonation constants from Figure 3, which are expected to electrostatically interact at the considered

(22) (a) Whitaker, J. E.; Haugland, R. P.; Prendergast, F. G. *Anal. Biochem.* **1991**, *194*, 330–344. (b) Baruah, M.; Qin, W. W.; Basarić, N.; De Borggraeve, W. M.; Boens, N. *J. Org. Chem.* **2005**, *70*, 4152–4157.
(23) Yao, S.; Schafer-Hales, K. J.; Belfield, K. D. *Org. Lett.* **2007**, *9*, 5645–5648.
(24) Velapoldi, R. A.; Tønnesen, H. H. *J. Fluoresc.* **2004**, *14*, 465–472.

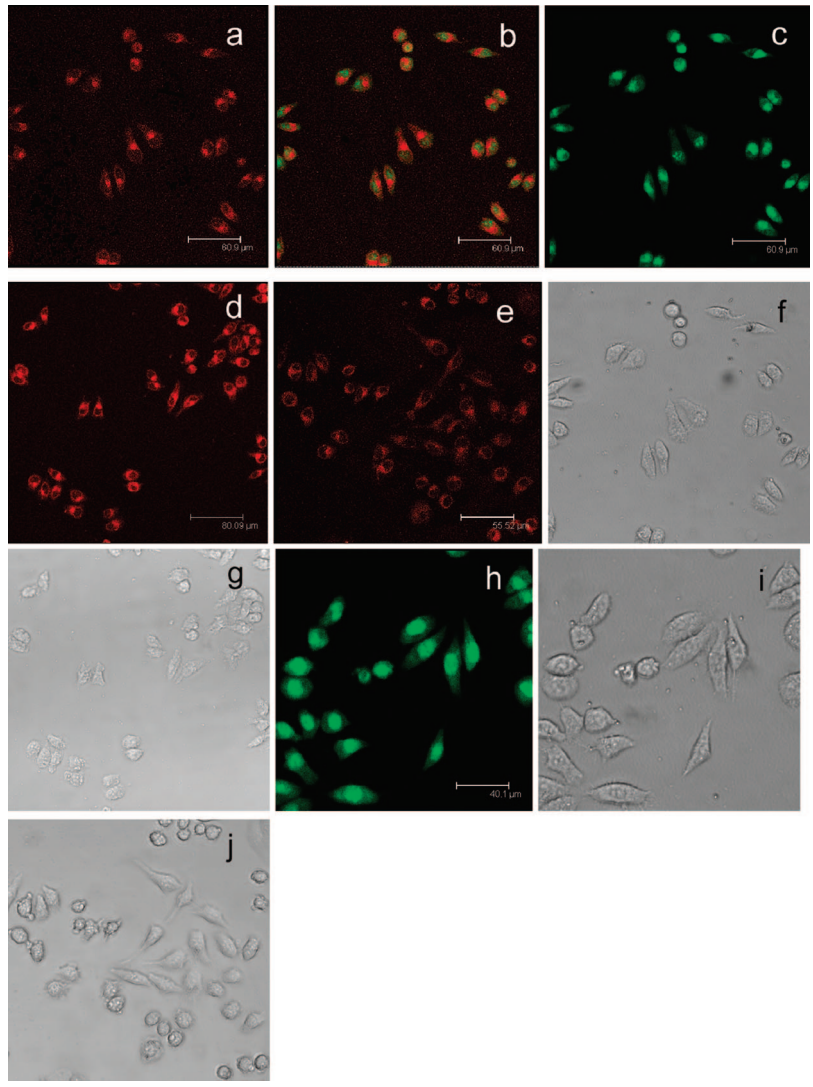


***Figure 6.*** Confocal fluorescence images of HepG2 cells. (1) HepG2 cells incubated with Tpy-Cy (1.0 $\mu$M) and AO (10 $\mu$g/mL) for 10 min pH 7.40, (a) and (c) were collected at $\lambda_{ex}$ = 633 and 488 nm respectively; (b) merged images of red (a) and green (c) channels; (f) bright-field image of (a). (2) HepG2 cells incubated with Tpy-Cy (1.0 $\mu$M): (d) 10 min pH 7.00; (g) bright-field image of (d); (e) 10 min pH 7.80. (3) HepG2 cells incubated with Tpy-Cy (1.0 $\mu$M) for 1 h at pH 7.40 and then incubated with AO for 10 min. (h) Collected at $\lambda_{ex}$ = 488 nm; (i) bright-field image of (h); (j) bright-field image of (e).

ionic strength. So more pH titrations in buffer solution at different ionic strengths were performed (NaCl: 0.05, 0.10, 0.15, 0.20 M). The results showed that there was no evident change in fluorescence emission intensity and wavelength (see Supporting Information). The analysis of fluorescence intensity changes indicated that the three basic sites of the probe shared the same value of the protonation constant and were independent, which based on molecular structure information.

The pH-dependent absorption spectra are presented in Figure 3c. With the increasing in peak of the alkaline form at 792 nm evolved with a well defined isosbestic point at 700 nm. The inset in Figure 3c shows the results of the nonlinear regression of the $\lambda$ at 792 nm according to a literature method,[23,25] affording a p$K_a$ value of ~7.10. The p$K_a$ value may also be calculated from the pH dependence of the total integrated fluorescence emission of Tpy-Cy excited at 648 nm.

The constants $K_a$ of Tpy-Cy was determined in aqueous buffered solution by fluorimetric titration as a function of pH using the fluorescence emission spectra. The expression of the steady-state fluorescence signal F as a function of the $H^+$ concentration has been derived for the case of a $n$:1 complex between $H^+$ and a fluorescent indicator,[22,26,27] eq 1

$$F = \frac{F_{max}[H^+]^n + F_{min}K_a}{K_a + [H^+]^n} \quad (1)$$

The fluorescence signals $F_{min}$ and $F_{max}$ at minimal and maximal $H^+$, respectively, and $n$ (the stoichiometry of $H^+$ binding to the probe). We get a p$K_a$ of 7.10, which is valuable for studying the near-neutral pH scale.

**Response to pH within Near-Neutral Range.** The choice of a fluorescent pH probe depends critically on the pH of the system one wants to investigate. And the p$K_a$ of the pH indicators must be well matched with the pH range of interest, because indicators have a usable fluorescence response in the range from ap-

(25) Billo, E. J. *Excel for Chemists, A Comprehensive Guide*; Wiley-VCH: New York, 1997; p 303.

(26) Qin, W. W.; Baruah, M.; Stefan, A.; Auweraer Van der, M.; Boens, N. *Chem. Phys. Chem.* **2005**, *6*, 2343–2351.

(27) Cielen, E.; Tahri, A.; Ver Heyen, A.; Hoornaert, G. J.; De Schryver, F. C.; Boens, N. *J. Chem. Soc., Perkin Trans.* **1998**, *2*, 1573–1580.

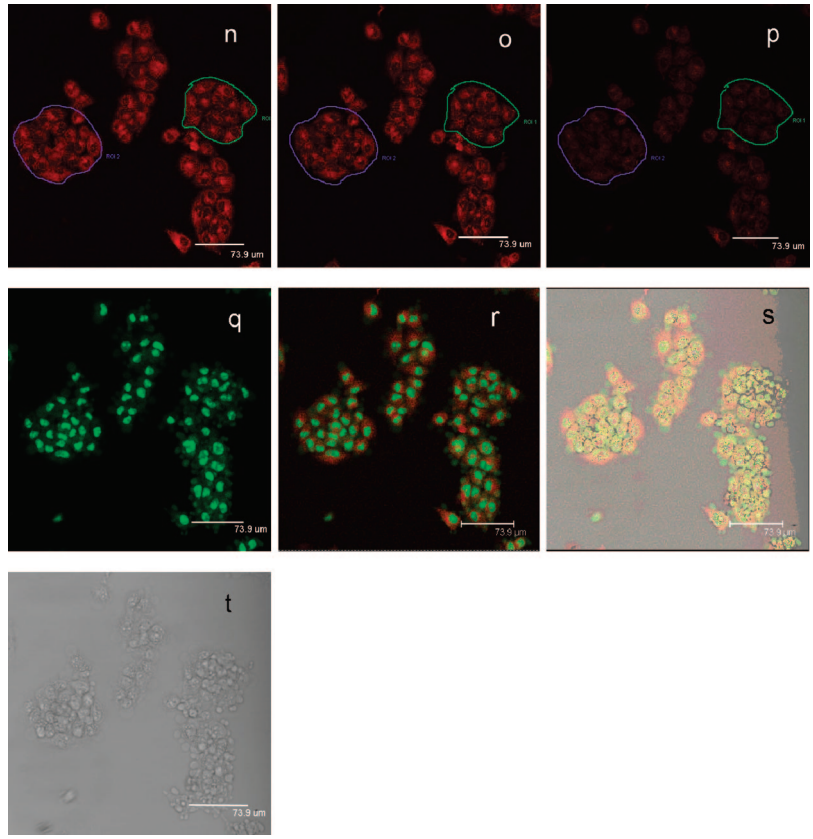


***Figure 7.*** Confocal fluorescence images of HL-7702 cells first cause cells to basify rapidly then acidify step by step; cells were incubated with Tpy-Cy (1.0 $\mu$M) and AO (10 $\mu$g/mL) for 10 min. (n) image of HL-7702 cells at pH 7.00; (o) image of HL-7702 cells at pH 7.40; (p) image of HL-7702 cells at pH 7.80; (q) was collected at $\lambda_{ex} = 488$ nm; (r) merged images of red (o) and green (q) channels; (s) merged images of red (o), green (q), and (t) bright-field channels; (t) bright-field image of (o).

***Table 1.*** Fluorescence Intensity of Parts n, o, and p of Figure 7 at Various pH Values

| data regions | pH 7.00 | pH 7.40 | pH 7.80 |
|---|---|---|---|
| ROI 1 | 36.04 | 24.14 | 10.95 |
| ROI 2 | 48.53 | 23.37 | 11.40 |

proximately 0.1 to 10 $K_a$. We focus on the near-neutral pH range because the normal physiological hydrogen ion concentration within very narrow limits and Tpy-Cy seems to achieve expected goal.

Standard fluorescence pH titrations were performed. There was a good linearity between fluorescence intensity and pH in the range from 6.70 to 7.90 (Figure 4). The regression equation was $F = 8812.2 - 1002.2 \times$ pH (inset 1 of Figure 4) with a linear coefficient of 0.9997. For the sake of eliminating the change of fluorophore concentration by photobleaching or change of the external environment, fluorescence intensity ratiometric data was provided (inset 2 of Figure 4). The regression equation was $I_{ratio} = 259.6 - 28.6 \times$ pH with a linear coefficient of 0.9901, which indicated that the probe could detect intracellular pH quantificationally within a narrow near neutrality scale.

**Test for Probe Selectivity.** On account that the amines can bind many metal cations in solution,[28] an additional important work of the probe was performed to determine whether other ions were potential interferents. Because of the complexity of the intracellular environment, the effects of adding proteins and other bioactive small molecules were also carried out. As shown in Figure 5, the Tpy-Cy showed excellent selectivity response to $H^+$ in the presence of metal ions, proteins, and bioactive small molecules.

**MTT Assay.** To evaluate cytotoxicity of the probe, we performed an MTT assay in HL-7702 cells with probe concentrations from 0.01 $\mu$M to 10.0 mM. The result showed IC50 = 1013 $\mu$M, which clearly demonstrated that the probe was of low toxicity to cultured cell lines under the experimental conditions at the concentration of 1.0 $\mu$M.

**Fluorescent Confocal Microscopy Image.** We applied Tpy-Cy to living HepG2 cells (human hepatocellular liver carcinoma cell line, first cause cells to acidify or basify rapidly and then incubated with Tpy-Cy 1.0 $\mu$M for 10 min at 37 °C and then washed with HEPES buffers at various pH values) to observe the changes of fluorescence brightness. The proton pumps in the cells did not rapidly reverse the effect on pH, and the buffering capacity of the cytoplasm was not strong enough to prevent the pH change. As predicted, we found that dye-loaded HepG2 cells (parts a, d, and e of Figure 6) showed different fluorescence intensity, which indicated that the probe could distinguish near-neutral pH fluctuations in cells. Bright-field transmission measurements after Tpy-Cy incubation confirmed that the cells were viable. Moreover, an acridine orange (AO) staining (parts c and h of Figure 6) was performed, which intuitively demonstrated that the probe was of low toxicity. (The

(28) (a) Silva, A. P.; Gunaratne, H. Q. N.; Gunnlaugsson, T.; Huxley, A. J. M.; McCoy, C. P.; Rademacher, J. T.; Rice, T. E. *Chem. Rev.* **1997**, *97*, 1515–1566. (b) Czarnik, A. W. *Acc. Chem. Res.* **1994**, *27*, 302–308.

time-dependence of the probe location in cells; see Supporting Information.)

Extensive studies had shown the probe Tpy-Cy: low toxicity, excellent membrane permeability, and good photostability. Meanwhile, the results proved that the probe located in cytoplasm and could distinguish near-neutral minor pH fluctuations in cells. We applied Tpy-Cy to living HL-7702 cells (human normal liver cells first cause cells to basify rapidly then acidify step by step; the cells were incubated with Tpy-Cy 1.0 $\mu$M for 10 min at 37 °C and then washed with HEPES buffers at various pH) to observe the changes of fluorescence brightness ([arts n, o and p of Figure 7). We selected two regions in visual field (ROI1 and ROI2 in parts n, o, and p of Figure 7), and the fluorescence intensity was calculated with confocal laser-scanning microscope respectively at various pH (Table 1). The data displayed that our probe depended on pH strongly and sensitively, and it was also showed that the probe, Tpy-Cy, was an efficient near-neutral fluorescent pH indicator. An AO staining was performed, which clearly demonstrated that the probe was of low toxicity to the cultured cell lines under the experimental conditions at the concentration of 1.0 $\mu$M (Figure 7q).

## Conclusion

In summary, we have developed a NIR fluorescent neutral-scale pH probe Tpy-Cy that is highly sensitive within the pH range of 6.70−7.90. The probe effectively avoids the influence of autofluorescence in biological systems and gives positive results when tested the near-neutral pH quantificationally both in aqueous solution and in living cells. The real-time imaging of cellular pH and the detection of pH in situ were achieved successfully. Furthermore, the results have demonstrated that the probe could be used to visualize intracellular minor pH changes with negligible background fluorescence. Therefore, the probe proposed here could be broadly applicable to the detection and quantification of minor pH changes in biological systems.

**Acknowledgment.** This work was supported by National Basic Research Program of China (973 Program, 2007CB936000), National Natural Science Funds for Distinguished Young Scholar (No. 20725518), Major Program of National Natural Science Foundation of China (No. 90713019), National Natural Science Foundation of China (No. 20575036), Important Project of Natural Science Foundation of Shandong Province in China (No. Z2006B09), and the Research Foundation for the Doctoral Program of Ministry of Education (No. 20060445002).

**Supporting Information Available:** Additional fluorescent confocal microscopy images, more materials of the article and $^{1}$H NMR, $^{13}$C NMR, MS, IR spectra of adduct 1−4. This material is available free of charge via the Internet at http://pubs.acs.org.

JA809149G